Wind and Structures, *Vol. 28, No. 4 (2019) 225-238*
DOI: https://doi.org/10.12989/was.2019.28.4.225

Numerical framework for stress cycle assessment of cables under vortex shedding excitations

Rafael O. Ruiz[*1,2], Luis Loyola[1a] and Juan F. Beltran[1b]

[1]Department of Civil Engineering, Universidad de Chile, Blanco Encalada 2002, Santiago, Chile
[2]Uncertainty Quantification Group, Center for Modern Computational Engineering, Facultad de Ciencias Físicas y Matemáticas, Universidad de Chile, Beauchef 851, Santiago, Chile

(Received March 30, 2018, Revised January 23, 2019, Accepted February 10, 2019)

Abstract. In this paper a novel and efficient computational framework to estimate the stress range versus number of cycles curves experienced by a cable due to external excitations (e.g., seismic excitations, traffic and wind-induced vibrations, among others) is proposed. This study is limited to the wind-cable interaction governed by the Vortex Shedding mechanism which mainly rules cables vibrations at low amplitudes that may lead to their failure due to bending fatigue damage. The algorithm relies on a stochastic approach to account for the uncertainties in the cable properties, initial conditions, damping, and wind excitation which are the variables that govern the wind-induced vibration phenomena in cables. These uncertainties are propagated adopting Monte Carlo simulations and the concept of importance sampling, which is used to reduce significantly the computational costs when new scenarios with different probabilistic models for the uncertainties are evaluated. A high fidelity cable model is also proposed, capturing the effect of its internal wires distribution and helix angles on the cables stress. Simulation results on a 15 mm diameter high-strength steel strand reveal that not accounting for the initial conditions uncertainties or using a coarse wind speed discretization lead to an underestimation of the stress range experienced by the cable. In addition, parametric studies illustrate the computational efficiency of the algorithm at estimating new scenarios with new probabilistic models, running 3000 times faster than the base case.

Keywords: enriched cable modeling; uncertainty quantification; cable fatigue; vortex shedding

1. Introduction

Cables has been widely used as critical load carrying members in many engineering application, including cranes, lifts, mine hoisting, bridges, cableways, electrical conductors, offshore mooring systems, among others (Chaplin 1999, Foster 2002, Sarkar and Taylor 2002). Typically, the internal structure of a cable is comprised by a series of components (wires) that can take different arrangements (different wire numbers and diameters) depending on the application. An adequate selection of components can lead a cable to have high axial strength and stiffness in relation to their weight, combined with a low flexural stiffness. This combination is achieved by using a large number of components, each of which is continuous throughout a cable’s length. When loaded axially, each component provides tensile strength and stiffness, but when deformed in bending, the components have a low combined bending stiffness (providing a bending deformation that is uncoupled from the axial response). To facilitate handling, it is necessary to ensure that a cable has some integrity as a structure, rather than being merely a set of parallel components. This characteristic is achieved by twisting the components together producing friction, bending and torsional moments between wires, characteristics that can significantly affect the integrity of the components (Chaplin 1999).

Considering that cables generally have high flexibility, long lengths, and low weight and damping, they tend to be excited to large amplitudes by minimal excitation amplitudes (Cluni *et al*. 2007, Flamand *et al.* 2014). Depending on the application, vibrations of cables are induced by wind, wind-rain, traffic and seismic events. These vibrations may induce axial fatigue (T-T fatigue) due to the fluctuation of the axial tension and bending fatigue (F-B fatigue) as a consequence of the combinations of an axial load and cyclic bending. The action of these two fatigue types, along with a harsh environment (that tends to corrode cable components), could induce cable damage as a result of the partial or complete rupture of some of their components. In the long term, this condition could compromise the safety and integrity of the structural system that damaged cables are part of (Cluni *et al*. 2007). Hence, the understanding of the interaction of the factors that govern the response of cables and their dependence on different operational conditions are essential to estimate cables service life at the design stage and to establish the appropriate inspection methods and discard criteria. Consequently, the service life of a cable can be greatly extended by following a planned program of installation, operation, maintenance, and inspection (Chaplin 2005).

*Corresponding author, Assistant Professor
E-mail: rafaelruiz@uchile.cl
[a] M.Sc. Student
E-mail: luis.loyola@ing.uchile.cl
[b] Assistant Professor
E-mail: jbeltran@ing.uchile.cl

http://www.techno-press.com/journals/was&subpage=7
ISSN: 1226-6116 (Print), 1598-6225 (Online)

In the particular case of transverse vibrations of stay cables and transmission line conductors, the fundamental fatigue failure is the cyclic stress bending due to wind vibration governed by the interwire fretting (relative slippage between adjacent wires) which is the primary mechanism responsible for individual wires deterioration (or even fractures) at the fixed ends (Chaplin 2005, Kalombo *et al.* 2016). Many works have been published on F-B fatigue problem (Wood and Frank 2009, Fadel *et al.* 2012, Winkler *et al.* 2015), however, there are still aspects of cable response under repeated loading that need to be clarified. Some of these aspects deal with: (1) transverse vibrations and fatigue life of damaged cables, (2) account for passive damping inherent in cables due to friction, (3) coupling between vibration modes (biaxial bending and torsion), and (4) the effect of uncertainties related to the excitation and the mechanical properties of the cable's material over the fatigue performance. It is important to note that these aspects can be studied conducting an experimental program especially designed for the purposes sought (particular cable construction, type of excitation, etc). However, the cost of fatigue tests (such as the rotative tensile test and rotative bending test) rapidly increases as the cable diameter gets larger, making in some cases the fatigue tests unfeasible (Cluni *et al.* 2007). Considering this drawback of experimental studies, the development of reliable, robust, and computational efficiency numerical model seems to be a promising computational tool to estimate bending fatigue of damaged cables and provide information that can be used to establish integrity-monitoring procedures during operational service and develop discard criteria.

The failure of cable components due to fatigue occurs in the region where there are restrictions on their vibratory motion such as the suspension clamps, spacer and dampers. In these localized regions, the cable undergoes rapid change in curvatures; thus a fiber-based model (accounting for axial strength energy only) is inadequate to accurately describe its mechanical behavior. In this kind of problems, a richer model for the cable/conductor should be developed in which the axial and bending properties need to be accounted for (Luongo and Zulli 2013). Note that increasing the model complexity also increases the computational cost employed to predict the cable behavior (which is an important factor to take into account if the model is evaluated several times to perform, for example, parametric analysis), then a balance between complexity and computational cost should be carefully evaluated. More details on this issue are presented later in Section 2.

Based on previous comments, the fatigue estimation in cables is a complex task since it requires not only an adequate cable model but also an adequate excitation model, which in fact has a stochastic behavior, i.e., wind excitation cannot be completely predicted since an aleatoric component is part of it. Moreover, the fatigue assessment relies on the estimation of the number of cycles at determined stress, indicating that the cable should be modeled dynamically, adding a dependency of the initial conditions, the tensile stress and the mechanical properties of the materials. The complexity of the problem increases even more since the information about the initial conditions of the cable are not known at the time that the wind starts exciting it, e.g., the cable can be vibrating by the action of another type of excitation (Giaccu *et al.* 2015). The tensile stress is also difficult to identify, it can be susceptible to changes in the loaded members, e.g., in stay bridges the tensile stress of a cable depends on the traffic load, which is time-varying (Argentini *et al.* 2016). In addition, the mechanical properties (e.g., density, Young´s modulus) of the elements employed in cables manufacturing depend on their thermal and mechanical history. Typically these values are tabulated and used as deterministic parameters when in reality represent an expected value. In this sense, the mechanical properties of the material employed in cables present variations reported between +/-5 and +/-10% of their nominal values (Jacinto *et al*. 2012). In general, the uncertainties related to the parameters mentioned above have an impact on the estimation of the dynamic response of the cable. However, and to the best of the author's knowledge, a limited attention has been paid to the quantification and propagation of these uncertainties in cables under wind-induced vibrations.

Some authors already recognized the need to tackle the cable vibrations from the stochastic perspective. Recently, Giaccu *et al*. studied the free response of a cable network assuming stochastic initial conditions, which are considered non-deterministic as a way to model the effect generated by the aeroelastic phenomenon. However, the authors limited the study to the malfunctioning identification of a cross-tie (Giaccu *et al*. 2015). In this sense, there is still the need to propose a more comprehensive and general models to incorporate uncertainties in the dynamical modelling of cables. Specifically, having a robust (account for uncertainties in mechanical properties of the cable, initial conditions, and tensile stress along with a realistic source-induced excitation) procedure based on stochastic modeling is essential for cable design and cable evaluation during operational service, and for developing discard criteria according to cable usage.

The aim of this work is to present an efficient computational framework to estimate the stress cycling behavior of cables subjected to wind-induced excitations. This framework takes into account the non-deterministic nature of the excitation and the limited knowledge about the mechanical properties of the cable, initial conditions (prior excitation), and its basal tensile stress. As a result, the framework could be used in the fatigue assessment. The excitation is limited to the mechanism of vortex shedding since it is the responsible of the predominant vibrations at low amplitudes, which affects directly the fatigue behavior (Cluni *et al*. 2007, Kumarasena *et al*. 2005) (more details on this issue are offered later in Section 3). However, the framework could be extended to incorporate other excitation sources (e.g., seismic excitations, traffic-induced vibrations, among others) or wind excitation models (e.g., recorded wind speed time-histories, artificial time-histories as realization of a specific power spectral density function). In particular, the work is focused on the efficient accounting of the variability associated to the wind speed in a particular time span and the uncertainties associated to the mechanical properties of the cable into the cycling stress estimation as well as the uncertainties associated to the tensile stress. The propagation of uncertainties is established adopting Monte Carlo simulations based on the concept of importance sampling, which is used here in such a way that different probabilistic models for the uncertain variables (wind speed, mechanical properties of the cable, initial conditions and basal tensile stress) could be evaluated without a significant additional computational burden. This is particularly important since the procedure allows the evaluation of the impact of these uncertainties on the dynamic response, giving information about which of the uncertainties could be neglected in this kind of problems (the procedure is fully described in Section 4). Another important aspect of the framework is that it allows the evaluation of a damaged cable with no extra computational cost. An alternative to model damaged cables consists on changing the Young´s modulus or the tensile stress, which can be easily introduced in the framework. Additionally, it is important to mention that the cable model used in the Monte Carlo simulations should considered both, identification of rapid changes in the cables curvature and the incorporation of the internal components characteristics (wires geometry and arrangements). This is a particularly important characteristic of the framework in order to keep a realistic modeling of the cable, reason why a beam-based high fidelity model is developed accounting for the effect of each wire (including the helix angle) on the axial stress of the cable. The details of this model is described later in Section 2.

This work presents the first effort to close an important gap in the modeling of wind-excited cables (oriented to fatigue prediction) by the incorporation of the model parameters (initial conditions, tensile stress, modal damping, and mechanical properties) and the wind velocity as uncertain variables in a framework that is computationally efficient and versatile (different probabilistic models can be evaluated with no additional effort). In summary, the procedure constitutes a powerful tool in the estimation of the axial stress range versus number of cycles curve experience by a cable due to: (*i*) it takes into account the variability associated to the wind speed, material properties and tensile stress, (*ii*) it uses a realistic cable model where the internal arrangements of components are considered, (*iii*) after a first run it allows to evaluate different tensile stress conditions, different mechanical properties, or even different cable damage stages without adding significant computational costs, and (*iv*) it is possible to evaluate not only the expected behavior but also the performance associated to some exceedance probability. All these characteristics are demonstrated in Section 5 through an illustrative example.

2. Enriched numerical model for cables

The core of the framework proposed is the use of a deterministic model to predict the dynamic behaviour of the cable subjected to dynamic excitations. As the cable model will be later employed to propagate uncertainties by adopting Monte Carlo simulations (that requires several evaluations of the cable model), it is necessary to select it by keeping an adequate balance between precision and computational burden.

One of the traditional and well-accepted numerical techniques, finite element (FE), presents several obstacles in the high fidelity modelling of cables. A high fidelity modelling involves 3D geometry that should account for interactions among cable components (complex multiple contact interactions between the inner wires). This interactions could induce modeling problems caused by bad convergence, potential loose of symmetry due to cable component failure, and important demand of computational resources (Nemov *et al.* 2010, Beltrán and Vargas 2012). Although some commercial FE codes (Knapp 1998, ABAQUS 1996, Hallquist 2006) have implemented numerical algorithms to overcome above convergence difficulties, problems related to high computational cost and convergence to the equilibrated solution in case of nonlinear problems, especially for large diameter ropes, still remain (Nemov *et al.* 2010). In this context, simpler models emerge as an alternative to estimate cyclic bending behavior of cables, providing information that can be used to perform fatigue assessment.

In this study, the cable is assumed to behave as a stiff cable, which means that the cable can undergo to large changes in curvature. Remember that important changes in the curvature are the main responsible of the fatigue phenomena, so the goal here is to establish a relative simple model able to capture the curvature in the cables components. To this end, the cable is modelled as a nonlinear beam under bending and axial load with Bernoulli´s kinematic hypothesis. Thus, a general 1D two-noded nonlinear beam element with two degrees of freedom (dof) per node is considered to discretize the length of the cable, Fig. 1(a) presents the scheme adopted for a beam element. In this way, the effects of the restrictions on the vibratory motion of the cable such as the suspension clamps, spacer and dampers on some of the interest characteristics of the response of a cable (stress/strain distribution; failures of the cable wires; dynamic parameters; and deformed configuration) under dynamic excitations can be accounted for (Luongo and Zulli 2013, Beltrán and De Vico 2015). Based on the finite element discretization of a cable, the equations of motion at time t are proposed to be written following the classical updated Lagrangian approach, in the framework of second order theory

$$\mathbf{M}\ddot{\mathbf{x}}+\mathbf{C}\dot{\mathbf{x}}+\left(\mathbf{K}+\mathbf{K}^{NL}\right)\mathbf{x}=\mathbf{f}\left(t\right) \tag{1}$$

where $\mathbf{M}$ is the mass matrix, $\mathbf{C}$ is the damping matrix, $\mathbf{f}\left(t\right)$ is the vector of nodal forces that depends on time t. Matrices $\mathbf{K}$ and $\mathbf{K}^{NL}$ are the linear and geometric nonlinear stiffness matrices respectively. The vector of nodal displacement is $\mathbf{x}$; and $\dot{\mathbf{x}}$, $\ddot{\mathbf{x}}$ are vectors of nodal velocity and nodal acceleration respectively. In the proposed formulation, both stiffness matrices are based on Hermite interpolation functions for the case of the bending rotations and transverse displacements. The vector of nodal forces

$\mathbf{f}(t)$ is related to wind-induced excitation on the cables. This vector will consider wind-cable interactions associated to Vortex Shedding using a probabilistic procedure (outlined in the following section) to describe and quantify the effect of the wind–induced excitation to the cable in the long term.

Refering to Eq. (1) and following the order of dof presented in Fig. 1(a), the linear stiffness matrix of each beam element is

$$\mathbf{K}_j = \overline{EI}\begin{bmatrix} \frac{12}{h_j^3} & \frac{6}{h_j^2} & -\frac{12}{h_j^3} & \frac{6}{h_j^2} \\ & \frac{4}{h_j} & -\frac{6}{h_j^2} & \frac{2}{h_j} \\ & sym & \frac{12}{h_j^3} & -\frac{6}{h_j^2} \\ & & & \frac{4}{h_j} \end{bmatrix} \quad (2)$$

while the local nonlinear stiffness matrix of each beam element presents the following expression

$$\mathbf{K}_j^{NL} = \sum_{i=1}^{M}\frac{t_i}{h_j}\begin{bmatrix} \frac{6}{5} & \frac{h_j}{10} & -\frac{6}{5} & \frac{h_j}{10} \\ & \frac{2h_j^2}{15} & -\frac{h_j}{10} & -\frac{h_j^2}{30} \\ & sym & \frac{6}{5} & -\frac{h_j}{10} \\ & & & \frac{2h_j^2}{15} \end{bmatrix}\cos(\eta_i) \quad (3)$$

In previous equations, h_j corresponds to the length of the j-th beam element while the equivalent bending stiffness $\overline{EI}$ is defined considering the Bernoulli´s kinematics hypothesis as

$$\overline{EI} = \sum_{i=1}^{M} E A_i r_i^2 \cos^3(\eta_i) + \sum_{i=1}^{M} E I_i \cos(\eta_i) \quad (4)$$

where M is the number of wires that form cable's cross-section. The expression presented in Eq. (4) comes from the use of different coordinate systems for the wires that compose the cable. A global coordinate system is located at the cable neutral axis (x-y coordinate system in Fig. 1(b)) while a local coordinate system is located at the centroid of each wire (x_i-y_i coordinate system in Fig. 1(b)). Then, the parameters A_i, r_i, I_i, and t_i correspond to the cross-sectional area, distance from cable neutral axis to the wire centroid in the y direction, inertia relative to a local axis x_i-y_i, and the axial load of the *i-th* wire that form of cable cross-section respectively. The $\cos(\eta_i)$ terms appearing to powers one and three account for the actual direction of each wire in the cable cross-section in which η_i is the helix angle of the *i-th* wire, as it is shown in Fig. 1(c). Note that not necessary all wires present the same helix angle, e.g., in the scheme presented in Fig. 1(b) the central wire has a different helix angle (in fact the angle is zero for this case) than the rest of wires. Note that the tensile force T in the cable is given by $T = \sum_{i=1}^{M} t_i \cos(\eta_i)$.

On the other hand, the local mass matrix of each beam element is given by

$$\mathbf{M}_j = \frac{\rho h_j}{420}\begin{bmatrix} 156 & 22h_j & 54 & -13h_j \\ & 4h_j & 13h_j & -3h_j \\ & sym & 156 & -22h_j \\ & & & 4h_j^2 \end{bmatrix} \quad (5)$$

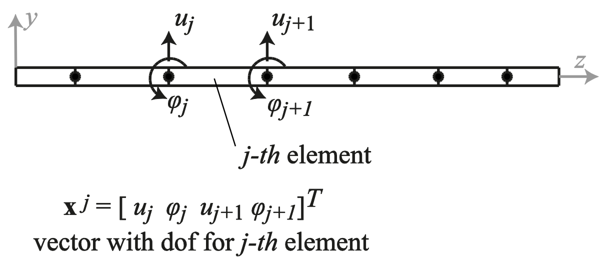

(a) Degrees of freedom employed in each beam element

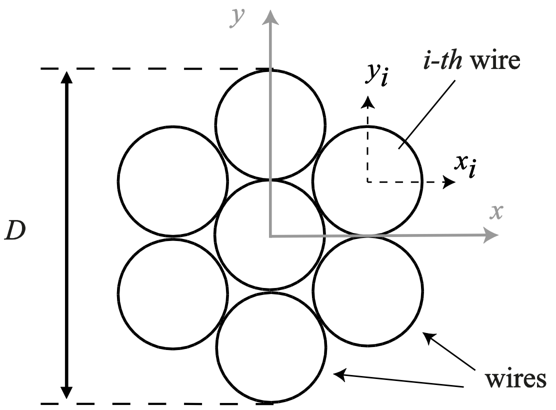

(b) Cable cross-section with local and global system of reference

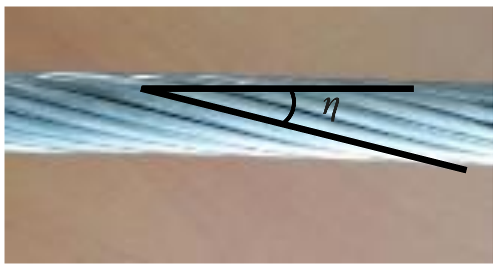

(c) Cable longitudinal view indicating the helix angle

Fig. 1 Scheme of the cable model

where ρ is linear density of the beam element. At this point, it is important to remark that the term enriched model is used in this study to indicate: (1) the capability to capture the cable's curvature and (2) the versatility to incorporate the geometry and arrangement of the cable's cross-section components (wires distribution and their respective helix angles).

The excitation force $\mathbf{f}(t)$ in Eq. (1) will be defined later in Section 3. Note that if the excitation and the initial condition are known, it is straightforward to integrate the equation in order to obtain the nodal displacement and rotation of the cable, e.g., adopting a traditional Dormain-Prince algorithm, Neumark Methods, amount others. Employing the Hermite interpolation function and nodal values of the displacement and rotation is possible to obtain the deflection of the cable at any point (any z coordinate, being z the longitudinal axis).

Approximating the cable curvature $\phi_o(z)$ by the second derivative of its deflection, the axial stress can be evaluated as $\sigma_{zz}(z) = -E\phi_o(z)y$, where y corresponds to the distance between a particular point in the cross-section of the cable and the neutral axis (please refers again to Fig. 1). For this case of study, the maximum radius of the cable ($y = D/2$) is used to estimate the contribution of the bending in the axial stress, which ultimately leads to the following expression of the axial stress valid in any element j of the mesh

$$\sigma_{zz}^{j}(z,t) = -E\frac{d^2\mathbf{N}_o(z)}{dz^2}\mathbf{x}^j(t)\frac{D}{2}\kappa \tag{6}$$

Here, $\mathbf{N}_o(z) \in R^{1x4}$ corresponds to a vector containing the Hermite interpolation functions, $\mathbf{x}^j(t)$ contains the time progression of the dof corresponding to the j-th element, and $\sigma_{zz}^{j}(z,t)$ corresponds to the axial stress of the j-th element at any position (z) and time (t). Note that κ corresponds to a correction factor that accounts for the helical configuration of a wire, which is equal to $\cos^2(\eta_{ext})$, being η_{ext} the helix angle of the outermost layer of the cable (Beltrán and De Vico 2015). Remember that large axial stress values are expected in areas where the transversal motion of the cable present significant restrictions, then it is possible to select the critical elements of the mesh according to the location of dampers, suspension clampers, spacers, etc. Once the critical elements are identified, the number of cycles (N) above certain level of axial stress (σ) can be accounted for a specific time window t_{int} by applying some cycle counting algorithm (e.g., level crossing cycle counting, rainflow counting method, among others, (Shinde *et al*. 2018)).

3. Excitation model

In terms of the dynamic excitations on cables, it is necessary to pointed out that these excitations can be produced by two different forcing mechanisms: (1) excitations transmitted by the movement of the clamped sections of the cable; and (2) forces directly applied on the cable body. The first group of excitations typically corresponds to excitation due to seismic activity or transmissibility product of excitations due to traffic or mobile loads in the adjacencies of the cable. On the other hand, the second group corresponds typically to excitations due to the wind-cable interactions, being the most relevant source of excitation in terms of the fatigue loading (as it was mentioned before in the introduction) (Cluni *et al*. 2007, Argentini *et al*. 2016). The wind-cable interaction can occur by different mechanisms: vortex shedding (resonance between the vortex shedding and the natural frequencies of the cable (Grouthier *et al*. 2014)), turbulent buffeting (high wind loads that change rapidly in time.), galloping (airflow creates uplift force around an unsymmetrical cross section (An1a *et al*. 2016)), and rain-wind vibrations (rainwater forms one or two rivulets under the influence of the airflow around the cable which change its aerodynamic shape in such a way that it is susceptible to vibrations, see for example (Guérard 2011, Li *et al*. 2016). Despite the different nature of the mechanism involved, the vortex shedding and turbulent buffering are the most important phenomena since they appear most of the time at regular wind speeds (Cluni *et al*. 2007, Wang *et al.* 2017).

3.1 Vortex shedding mechanism

Although the mechanisms described above have been widely studied in the past, their modelling still represent a challenging task since it requires a lot expertise and computational resources in the coupling of the solid and fluid equation of motions. However, there are some special cases for which the fluid-structure interaction can be represented by simplified models, e.g., assuming a constant wind speed (pure vortex shedding) (Carberry *et al*. 2001) or imposing a variance defined by a power spectral density over a mean wind speed (turbulent buffeting) (Cluni *et al*. 2007, Wang *et al.* 2017). Those models can adequately represent the behavior of the cable in short periods of time but they do not necessarily represent the real behavior in a long term. In that sense, it is still needed a more adequate description of the wind speed, incorporating a probabilistic procedure to describe and quantify the effect of the coexistence of those mechanisms. The procedure proposed in this study, however, assumes a pure vortex shedding as a source of excitation since it is the phenomenon presented the most part of the time. The mechanical model for vibrations induced by vortex shedding is shown in Fig. 2, where it is presented a double clamped cable subjected to an air flow at a constant speed v that generates transversal vibrations $u(z,t)$.

The use of vortex shedding as an excitation mechanism can be validated evaluating the range of the expected wind speed together with the transversal geometry of the cable. The wind speed reported in the literature indicates that the most frequent speed lies in a region between zero and 14 m/s (Seguro and Lambert 2000, Carta *et al*. 2009, Ge *et al*. 2018). These values are important to identify the regime of the fluid (air for this case) over the cable. Typically, the

Reynolds number is used as an indicator of this regime, and it is defined as

$$\mathrm{Re} = \frac{\rho v D}{\mu} \tag{7}$$

where ρ defines the air density (1.225 kg/m^3) , D the cable diameter and μ the air viscosity. In this sense, Reynolds numbers between $1\text{x}10^4$ and $3\text{x}10^5$ indicate the presence of vortex shedding, which is the case for common cable diameters and wind speed. Furthermore, in this range the Strouhal number takes a relatively constant value equal to 0.2 enforcing a shedding frequency Ω (Kumarasena *et al.* 2005) given by

$$\Omega = \frac{0.2 v}{D} \tag{8}$$

Finally, the total lifting force (excitation force in the *y*-direction) can be expressed by (Facchinetti *et al.* 2004, Carberry *et al.* 2001, Lipecki and Flaga 2013)

$$f(t) = \frac{1}{2} c_l \, \rho D L v^2 \cos(\Omega t) \tag{9}$$

where c_l corresponds to the lifting coefficient, estimated in similar problems around 0.3.

3.2 Probabilistic wind description

The previous vortex shedding model is adequate for constant fluid speeds. However, this assumption is non-realistic for the case of wind-induced vibrations since the wind speed is usually described adopting a probabilistic model. The description and characterization of the wind speed represent an important source of information for different fields like meteorology, climatology and wind energy. In this sense, there is an important effort towards to generate wind models to adequately predict wind direction and speed. Many researchers have been proposed different probabilistic models to describe the wind speed behaviour, being the Weibull distribution one of the most common Probability Density Functions (PDFs) used to this purpose (Carta *et al.* 2009, Chiodo and De Falco 2016). This PDF is presented in the following equation

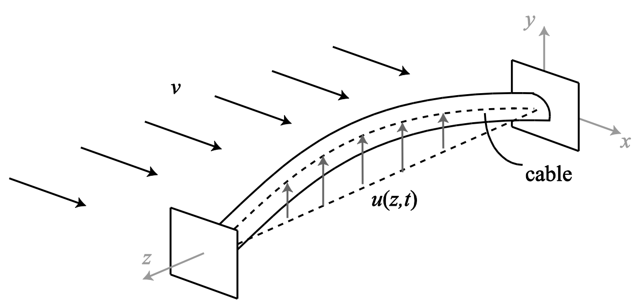

Fig. 2 Mechanical model to study wind-induced vibrations in cables due to vortex sheeding phenomenon

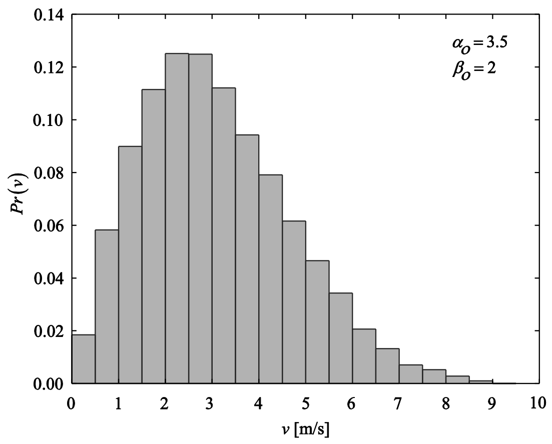

Fig. 3 Typical histogram associated to the wind speed

$$p(v) = \frac{\beta_o}{\alpha_o} \left(\frac{v}{\alpha_o} \right)^{\beta_o - 1} e^{-\left(\frac{v}{\alpha_o} \right)^{\beta_o}} \tag{10}$$

In Eq. (10), α_o and β_o correspond to shape parameters that could be related to meteorological and geographic location of a specific area, respectively. In this context, several research institutes, meteorological stations and researchers have been optimized Eq. (10) for specific regions, i.e., identification of α_o and β_o based on direct measurements of the wind speed during a significant period of time, usually yearly periods (Carta *et al*. 2009, Seguro and Lambert 2000).

Additionally to the optimized PDF, it is also possible to find histograms of the wind speed based on measurements. In this case, each bin of the histogram represents the probability that a speed belonging to the bin occurs. Note that the histogram can be obtained either by manipulating directly the available measurements or by generating samplings from the PDF presented in Eq. (10). An example of these histograms is presented in Fig. 3 by using a Weibull distribution with $\alpha_o = 3.5$ and $\beta_o = 2$. In this illustration, the discretization of the wind speed corresponds to intervals of 0.5 m/s, generating a total of 20 bins between 0 and 10 m/s, where the height of each bin corresponds to the probability to have a wind speed inside the bin.

Once the probabilistic description of the wind speed is established, it is possible to incorporate the wind model as the excitation in Eq. (1) to estimate the dynamic response of the cable (the following section offers details on this procedure). However, another important issue has to be taken into consideration dealing with the identification of an adequate time span to integrate Eq. (1). In other words, it is necessary to identify the maximum duration (t_{int}) for which the wind speed described in the histogram can be considered constant. Based on the available information found in (Matsumoto *et al.* 2003, Harper *et al*. 2010), it is decided to establish 60s as an adequate time span.

4. Stress cycles assessment under uncertainties

In this section, the probabilistic model for the wind speed and the uncertainties associated to the model parameters are propagated to estimate the number of cycles at a particular axial stress. Note that model parameters here refer to: geometry, initial conditions, tensile stress, modal damping, and mechanical properties.

First, the deterministic case is discussed in order to formalize the notation, which is extended later to the case where the uncertainties are taking into account. Note that if the model parameters and the wind speed are known then is straightforward to integrate Eq. (1) between zero seconds and t_{int} to identify the displacement and rotation of each node (cable discretization). This result can be used in Eq. (6) to identify the time history of the axial stress at any point of the cable. Afterward, the number of cycles (N_i) that exceeds a specific axial stress (σ_i) could be computed applying, for example, a rainflow counting method as it was mentioned in Section 2. In this sense, a vector $\boldsymbol{\sigma}_{ref} = [\sigma_1 \quad \sigma_2 \quad \cdots]^T$ is defined containing different values of axial stress, while another vector $\mathbf{N}_c = [N_1 \quad N_2 \quad \cdots]$ is defined containing the number of cycles that exceeds the respective axial stress value. Here, the vector $\mathbf{N}_c$ depends on the wind speed velocity v, the time integration t_{int}, and the model parameters of the cable. For the sake of simplicity, the vector $\mathbf{N}_c$ from now on is denoted as the function $\mathbf{N}_c(\boldsymbol{\theta}, v, t_{int})$, where $\boldsymbol{\theta}$ denotes a vector containing the model parameters.

Now, if $\boldsymbol{\theta}$ contains the model parameters, but these parameters are uncertain, it is possible to propagate these uncertainties by applying the total probability theorem such that

$$E\left[\mathbf{N}_c\left(v, t_{int}\right)\right] = \int_{\Theta} \mathbf{N}_c\left(\boldsymbol{\theta} \middle| v, t_{int}\right) p\left(\boldsymbol{\theta}\right) d\,\boldsymbol{\theta} \tag{11}$$

where $p(\boldsymbol{\theta})$ corresponds to the PDF assigned to the model parameters $\boldsymbol{\theta} \in \Theta$, and $E[\mathbf{N}_c(v, t_{int})]$ corresponds to the expected number of cycles that exceed $\boldsymbol{\sigma}_{ref}$ for a known wind speed and time integration. Please note that $\mathbf{N}_c(\boldsymbol{\theta}|v, t_{int})$ is used here instead $\mathbf{N}_c(\boldsymbol{\theta}, v, t_{int})$ to explicitly indicate which parameters are considered uncertain (left side of the vertical bar) and which are known (right side of the vertical bar), this notation will be used extensively in this work.

Now, it is necessary to include the uncertain nature of the wind speed v. As it is mentioned in Section 3.2, the wind speed is usually described through a Weibull distribution, i.e., the distribution presented in Eq. (10) where the wind speed v belongs to a space V. Ultimately, this variability in wind model can be propagated in the same fashion as Eq. (11), leading to

$$E\left[\mathbf{N}_c\left(t_{int}\right)\right] = \int_V \int_{\Theta} \mathbf{N}_c\left(\boldsymbol{\theta} \middle| v, t_{int}\right) p\left(\boldsymbol{\theta}\right) p\left(v\right) d\,\boldsymbol{\theta}\, dv \tag{12}$$

Here, Eq. (12) assumes that the model parameter vector and the wind speed are independent since there is not strong evidence in the literature to assume a correlation between the variables. This equation leads to the estimation of the expected number of cycles $E[\mathbf{N}_c(t_{int})]$ that exceeds $\boldsymbol{\sigma}_{ref}$ (after propagating uncertainties related to model parameters and wind speed) in a period of time defined by the integration time t_{int}. Please note that the number of cycles can be scaled to identify the number of cycles in any other period of time T_{life} only by multiplying Eq. (12) by the ratio T_{life}/t_{int} . Another interesting metric could be also implemented, for example the probability of $\mathbf{N}_c(\boldsymbol{\theta}, v | t_{int})$ be greater than certain threshold, as it is indicated in Eq. (13). This metric could be used in risk evaluation by identifying the threshold associated to specific probability of exceedance or in failure analysis by identifying the probability to exceed the number of cycles associated to the cable or wire rupture.

$$\Pr\left(\mathbf{N}_c\left(\boldsymbol{\theta}, v \middle| t_{int}\right) > \mathbf{N}_{threshold}\right) = P_o \tag{13}$$

Different methods can be used to solve Eqs. (12) and (13), being stochastic simulation-based methods the most general and unconstrained approach, allowing the used of any given probabilistic model for $p(\boldsymbol{\theta})$, a detailed information on this issue is presented next.

4.1 Computational details

The focus of this section is to introduce an efficient method to solve the probabilistic integral presented in Eq. (12). This equation can be generalized in the following form

$$E\left[g\right] = \int_{\Theta_o} g\left(\boldsymbol{\theta}_o\right) p\left(\boldsymbol{\theta}_o\right) d\,\boldsymbol{\theta}_o \tag{14}$$

for example, by assembling the model parameter vector and the wind speed in a new vector $\boldsymbol{\theta}_o = [\boldsymbol{\theta} \quad v]$ that follows the distribution $p(\boldsymbol{\theta}_o) = p(\boldsymbol{\theta})\, p(v)$. The generalized stochastic equation could be solved by applying a standard Monte Carlo simulation. However, the method usually demands significant computational cost since it requires multiples evaluation of the function $g(\boldsymbol{\theta}_o)$. To alleviate this computational demand it is proposed to employ the importance sampling technique since it requires less evaluations of $g(\boldsymbol{\theta}_o)$ to keep the same accuracy in the estimation of $E[g]$. The base of the method is to draw a set of samples $\{\boldsymbol{\theta}_o^i,\ i = 1, \ldots, K\}$ from a proposal density $q(\boldsymbol{\theta}_o)$ to estimate the probabilistic integral as

$$E\left[g\right] \approx \frac{1}{K} \sum_{i=1}^{K} \frac{g\left(\boldsymbol{\theta}_o^i\right) p\left(\boldsymbol{\theta}_o^i\right)}{q\left(\boldsymbol{\theta}_o^i\right)} \tag{15}$$

The proposal density $q(\boldsymbol{\theta}_o)$ should be selected in such a way that fully covers the region where the integrand of Eq. (14) is significant. Moreover, it is possible to demonstrate that the optimal proposal density corresponds to a distribution that is proportional to the integrand (Lutes and Sarkani 1997). Additionally, the use of the importance sampling technique introduces certain degree of freedom in the estimation of the cable performance under different probabilistic scenarios without incurring in a significant computational cost. Note that in Eq. (14) the function $g(\boldsymbol{\theta}_o)$ corresponds to the estimation of the number of cycles at certain level of axial stress in the cable $\mathbf{N}_c(\boldsymbol{\theta},v|t_{int})$. The estimation of this parameter for a given model parameter $\boldsymbol{\theta}$ and wind speed v involved the time integration of Eq. (1), which requires certain computational cost (typical values are not reported here since the integration cost is problem dependent). In order to propagate uncertainties by applying the importance sampling technique, the function $\mathbf{N}_c(\boldsymbol{\theta},v|t_{int})$ should be evaluated in each sample drawn from $q(\boldsymbol{\theta}_o)$, increasing the computational cost in a factor of *K*. However, the versatility of the procedure arises from the fact that the evaluation of $\mathbf{N}_c(\boldsymbol{\theta},v|t_{int})$ is independent of $p(\boldsymbol{\theta}_o)$ since the samples are drawn from $q(\boldsymbol{\theta}_o)$. Then, a new probabilistic model for the cable $p(\boldsymbol{\theta}_o)$ could be evaluated by computing the Eq. (15) without the need to compute again the whole set of $g(\boldsymbol{\theta}_o^i)$. This versatility will be revisited later in the implementation example to show the efficiency of the procedure to estimate the cable performance under different tensile stresses.

An important limitation of this procedure lies in the selection of the proposal density $q(\boldsymbol{\theta}_o)$. This density should cover at least the space where the integrand of Eq. (14) presents its maximum, narrower distributions lead to results that are not representative of the integrand, while much wider distributions are inefficient since only few samples will be in the integrand relevant space. Here, it is important to mention that the expected variation of the cable model parameters $\boldsymbol{\theta}$ is not as significant as the variation in the wind speed *v*. Note that an important variation in the wind speed model is desirable to allow not only the imposition of any wind speed distribution but also to allow the performance estimation of the cable under a deterministic wind speeds. The later condition is particularly relevant to use the framework to support experimental results, which are conducted usually at constant wind speed (Facchinetti *et al.* 2004, Ge *et al.* 2018). Additionally, the use of deterministic wind speeds is also relevant to study the cable behaviour under resonance condition.

For the reasons mentioned above, it is decided to implement the importance sampling method only for the model parameters $\boldsymbol{\theta}$, such that

$$E\left[\mathbf{N}_c\left(v,t_{int}\right)\right] \approx \frac{1}{K}\sum_{i=1}^{K}\frac{\mathbf{N}_c\left(\boldsymbol{\theta}^i\left|v,t_{int}\right.\right)p\left(\boldsymbol{\theta}^i\right)}{q\left(\boldsymbol{\theta}^i\right)} \tag{16}$$

and to use a histogram-weighted wind speed to propagate the uncertainties related to *v*, then Eq. (12) can be approximated to

$$E\left[\mathbf{N}_c\left(t_{int}\right)\right] \approx \sum_{i=1}^{K} E\left[\mathbf{N}_c\left(v_j,t_{int}\right)\right]\Pr\left(v_j\right) \tag{17}$$

Finally by matching Eqs. (16) and (17), a general solution for any time span (T_{life}) is obtained

$$E\left[\mathbf{N}_c\right] \approx \left(\sum_{j=1}^{M}\left(\frac{1}{K}\sum_{i=1}^{K}\frac{\mathbf{N}_c\left(\boldsymbol{\theta}^i\left|v_j,t_{int}\right.\right)p\left(\boldsymbol{\theta}^i\right)}{q\left(\boldsymbol{\theta}^i\right)}\right)\Pr\left(v_j\right)\right)\frac{T_{life}}{t_{int}} \tag{18}$$

The above equation could be evaluated considering the current properties of a cable, i.e., cable properties can be regularly updated after a specific service time by implementing some parameter identification technique. In this way, the evaluation of Eq. (18) considers the degradation of the mechanical properties due to bending fatigue; thus $\boldsymbol{\sigma}_{ref}$ and $E[\mathbf{N}_c]$ values could be plotted and compared to any fatigue model, e.g., the traditional S-N (Stress-Number of cycles) fatigue curve (Kwofie 2001) for checking failure purposes

$$\frac{\Delta\sigma}{\Delta\sigma_s} = \left(\frac{N}{N_s}\right)^{-\left(\frac{1}{b}\right)} \tag{19}$$

where $\Delta\sigma$ is the peak-to-peak value of the axial stress that induces a failure in *N* cycles, while $\Delta\sigma_s$ is the maximum delta stress that guarantees infinite life (in terms of axial fatigue).

4.2 Algorithm

Before describing the procedure to identify the number of cycles vs. axial stress it is necessary to make some comments on how to define the initial conditions. The mechanical model of the cable requires two sets of initial condition, displacement and velocities. It is well-known that the response of any linear system can be describe as the linear combination of their vibration modes $\{\boldsymbol{\phi}_k,\ k=1,\ldots,n\}$. Then, the initial displacement could be expressed as

$$\mathbf{x}_o = \frac{\sum_{k=1}^{n}\boldsymbol{\phi}_k\alpha_k}{\left\|\sum_{k=1}^{n}\boldsymbol{\phi}_k\alpha_k\right\|_\infty}\beta \tag{20}$$

In the above expression, it is important to normalize the vibration modes respect to the maximum value associated to the displacements, such that β can be associated to the maximum physical displacement of the cable vibrating in *n*-modes, each of them weighted with a factor α_k. On the other hand, the set of initial velocities could be considered either in the same fashion or null (i.e., the initial condition is assumed in a cycle of maximum deflexion), depending on the designer criteria.

The algorithm to quantify the number of cycles for a specific axial stress levels is summarized and presented in the following paragraphs. Additionally, an overview is presented in Fig. 4.

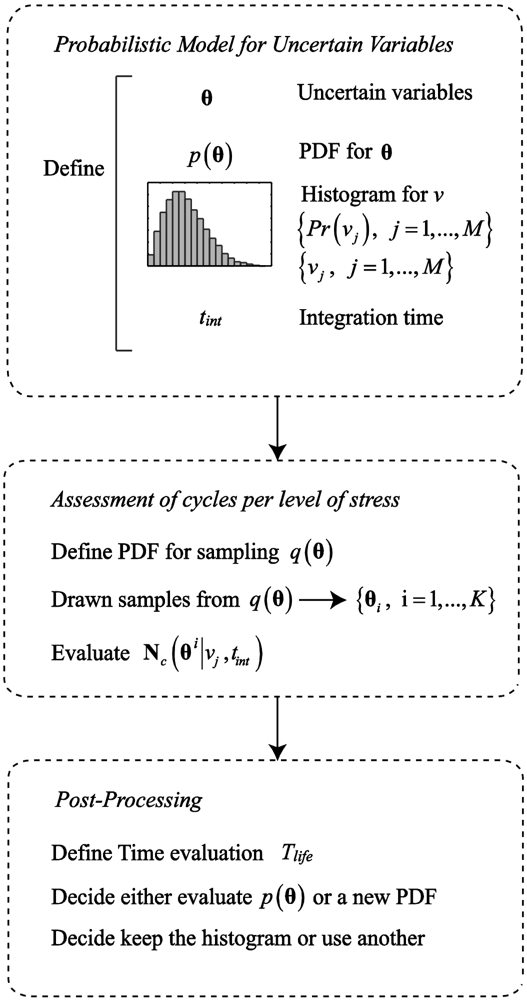

Fig. 4 Algorithm for the robust estimation of the number of cycles per stress level

Probabilistic models for uncertain variables (First Step in Fig. 4): First, it is necessary to define the model parameters that are considered uncertain. In this work, it is assumed that only the tensile force (T), the Young's modulus (E), and the damping ratio for each mode (ξ_k) are uncertain. For the numerical integration, it is also necessary to define the values α_k and β used in Eq. (20) to define the initial conditions; these parameters are also considered as uncertain variables. In this sense, the vector $\boldsymbol{\theta}$ containing the uncertain variables is defined as $\boldsymbol{\theta} = [T \quad E \quad \xi \quad \alpha \quad \beta]^T$, with $\alpha = [\alpha_1 \quad \cdots \quad \alpha_n]$ and $\xi = [\xi_1 \quad \cdots \quad \xi_n]$. Based on the available knowledge of $\boldsymbol{\theta}$ (mean, variance, bounds of confidence), it is required to define a proper probability density function $p(\boldsymbol{\theta})$. On the other hand, the wind speed should be also defined by adopting a representative wind model. The most important data correspond to the histogram of the wind speed. Here, it is possible to work either with a given histogram or with a histogram that represents the typical Weibull distribution presented in Eq. (10). It should be pointed out that regardless the histogram is prescribed or obtained from Eq. (10), it should be carefully normalized, i.e., the sum of all normalized bin frequencies should be one. Then, the height of the bin directly corresponds to the probability to obtain the velocity associated to that bin $\Pr(v_j)$. The histogram chosen has to be representative of the wind speed for long periods of time, typically one year. Note that as a result of the histogram identification, two sets of data are available: $\{v_j,\ j=1,...,M\}$ and $\{\Pr(v_j),\ j=1,...,M\}$. Another important parameter to be identified is t_{int}, that represents the credible time span in which the wind speed could be considered constant.

Assessment of cycles per level of stress (Second Step in Fig. 4): The second step consists in the computation of $\mathbf{N}_c(\boldsymbol{\theta}^i | v_j, t_{int})$. In this stage, it is necessary to define the probability density function $q(\boldsymbol{\theta})$. The selection of $q(\boldsymbol{\theta})$ should be made taking into consideration two aspects: (i) it should be much wider than $p(\boldsymbol{\theta})$ and (ii) it should be centred as close as possible to the maximum of the integrand of Eq. (14). If no information is available, it is possible to choose $q(\boldsymbol{\theta})$ equal to $p(\boldsymbol{\theta})$ but with a greater variance of its variables. After defining $q(\boldsymbol{\theta})$, it is necessary to draw K samples from it, identifying the set $\{\boldsymbol{\theta}^i,\ i=1,...,K\}$, to later perform K-by-M calculations to evaluate $\mathbf{N}_c(\boldsymbol{\theta}^i | v_j, t_{int})$. This step is the most expensive in terms of computational time.

Post-processing (Third Step in Fig. 4): The last step consists in the evaluation of Eq. (18). Here, the user can decide either to evaluate the same probabilistic model $p(\boldsymbol{\theta})$ defined previously or to select a different model. Additionally, it is possible to select a different histogram for the wind speed (keeping in mind that it has to have the same number of bins) or a different evaluation time T_{life}. All these parameters are independent of $\mathbf{N}_c(\boldsymbol{\theta}^i | v_j, t_{int})$, then the computational cost associated to the evaluation of a new scenario, i.e., different T_{life}, $p(\boldsymbol{\theta})$ or different wind histogram does not represent an additional computational burden.

5. Illustrative example

To illustrate the proposed framework, a 15 mm diameter high-strength steel strand composed by 7 wires is considered for the analysis of contribution of the vortex shedding-induced vibrations on the bending fatigue. The helix angle η (rotation of the local longitudinal axis relative to the global longitudinal axis of the cable) of the outer wires is approximately 10° (Bean 2006), see for instance Fig. 1. The core and the outer helical wires are assumed linear elastic (Qi 2013) with elastic modulus E equal to 200 GPa. The guaranteed ultimate tensile strength (G*UTS*) of the cable is equal to 250 kN (with a yield stress equal to 1600 MPa) and the pretension force is set equal to 40% of *GUTS* (i.e., 100 kN). For modelling purpose, a 20 beam elements (FE) model of the cable is used considering a cable length L equal to 15 m.

The excitation force in Eq. (1) is adopted based on the model presented in Eq. (9). The dynamic problem is solved by a traditional Dormain-Prince integration algorithm. For this case of study, the cable is considered fixed at the ends (following the scheme presented in Fig. 2), place that is selected to compute the axial stress (maximum radius of the cable is used to estimate the axial stress) since it corresponds to the location where wire failures occur due to fatigue phenomenon (Chaplin 2005, Kalombo *et al*. 2016). Finally, the number of cycles ($\mathbf{N}_c$) above certain level of axial stress ($\boldsymbol{\sigma}_{ref}$) is accounted for a specific time window t_{int} (as it was argued in Section 3.2, 0 to 60s time windows is chosen to perform the integration).

The framework proposed in this study starts (see for instance Fig. 4) with the definition of the probabilistic model $p(\boldsymbol{\theta})$. The uncertain variables are grouped in vector $\boldsymbol{\theta}$ as it was mentioned before in Section 4.2, then the probabilistic model $p(\boldsymbol{\theta})$ corresponds to a multivariate PDF. This probabilistic model is described next along with the nominal characteristics of the cable (presented in Table 1). The tensile force (T) and the elastic modulus (E) are considered independent Gaussian variables with mean equal to the nominal values, both with 10% of coefficient of variation. The damping ratio is considered as a lognormal distribution with median equal to 0.001 (similar values have been used before in other works (Argentini *et al*. 2016, Raeesi *et al*. 2014)) and 10% of coefficient of variation for each mode (all damping ratios are considered uncorrelated). The initial conditions are considered imposing Eq. (20) where the weights α_k are defined by employing a uniform distribution between [0,1] and where β is defined by a Gaussian distribution with mean equal to one third of the cable's diameter and coefficient of variation equal to 10% (value that is in agreement with observations, see for instance (Raeesi *et al.* 2014)). It is important to note that the probabilistic model employed in this illustrative example is arbitrary. In that sense, the probabilistic model adopted here has the intention to illustrate the capabilities of the numerical procedure proposed rather than to simulate the performance of a cable under service condition. More realistic analysis, however, can be performed considering a probabilistic model based on the information available about the confidence of the variables (elastic modulus, tensile force, damping ratios, initial conditions) involved in the problem.

The wind model is established defining a Weibull distribution presented in Eq. (10) with $\alpha_o = 6$ and $\beta_o = 2$ (both arbitrary chosen for this example, however the wind model could be selected based on the information available for a specific location, for instance the wind models presented in (Carta *et al.* 2009). The wind speed histogram is defined by using 13 bins (M =13 in Fig. 4) to have a speed discretization approximately equal to 1 m/s (value that have been previously used for structural health monitoring of suspension bridges (Comanducci *et al*. 2015)), however, different discretizations are studied later in Section 5.2. to identify their effect on the fatigue prediction.

Table 1 Nominal characteristics of the cable

Length	15 m
Elastic modulus	200 Gpa
Tensile force	100 kN
Number of wires	7
Diameter of the strand	15 mm

The second step in the procedure corresponds to select the proposal density $q(\boldsymbol{\theta})$ to sampling from. This PDF should be carefully selected since it is required to be broader than $p(\boldsymbol{\theta})$. The broader $q(\boldsymbol{\theta})$ the greater is the flexibility to select a different probabilistic model $p(\boldsymbol{\theta})$ for the uncertain variables. It is important to point out that the idea behind sampling from a different PDF (sampling from $q(\boldsymbol{\theta})$ instead of $p(\boldsymbol{\theta})$) relies on the versatility to evaluate new probabilistic models (different $p(\boldsymbol{\theta})$) without significantly increase the computational burden. Note for instance that if $q(\boldsymbol{\theta})$ is selected equal to $p(\boldsymbol{\theta})$, Eq. (18) corresponds to the case of a Direct Monte Carlo method, i.e., Eq. (18) can be wrote as

$$E\left[\mathbf{N}_c\right] \approx \left(\sum_{j=1}^{M} \left(\frac{1}{K} \sum_{i=1}^{K} \mathbf{N}_c\left(\boldsymbol{\theta}^i \middle| v_j, t_{int}\right) \right) \Pr\left(v_j\right) \right) \frac{T_{life}}{t_{int}} \quad (21)$$

For the illustrative example presented, $q(\boldsymbol{\theta})$ is selected keeping the same PDF $p(\boldsymbol{\theta})$ except for the tensile force (T) and the elastic modulus (E) that are assumed as independent Gaussian variables with mean equal to the nominal values, but now with 100% of coefficient of variation for each variable. The reason to wider the probabilistic model only for T and E is based on the intention to evaluate different service condition of the cable studied. Other probabilistic models for the rest of the uncertain variables (damping ratios, initial conditions) could be implemented in the same fashion but for the sake of simplicity it is decided to evaluate only different scenarios for T and E.

After defined the probabilistic models, 10000 samples are drawn from $q(\boldsymbol{\theta})$, whereby the function $\mathbf{N}_c\left(\boldsymbol{\theta}^i \middle| v_j, t_{int}\right)$ is evaluated 10000 times for each wind speed. This process takes close to 600s in order to run the whole set of data, where the results are saved and used in the post processing stage (step 3 in Fig. 4). In the post processing stage, the results obtained are used to evaluate the cable response under the interested probabilistic models $p(\boldsymbol{\theta})$ for the uncertain variables and $\Pr(v)$ for the wind speed. More details are offered in Section 5.3 where it is discussed the versatility of the procedure to evaluate a different $p(\boldsymbol{\theta})$ and $\Pr(v)$ taking advantage of the previous calculation of $\mathbf{N}_c\left(\boldsymbol{\theta}^i \middle| v_j, t_{int}\right)$. Additionally, the period of time T_{life} in which the analysis is conducted can be selected ad hoc. For the case presented all results corresponds to a period of one year.

5.1 Effect of the uncertainties in the model parameters

In Fig. 5 the impact of the uncertainties associated to the elastic modulus, tensile force, damping ratios and initial conditions on the number of cycles for particular values of stress ranges is presented. For the case in which all uncertainties are accounted for simultaneously, stress range decreases as the number of cycles increases. For a low number of cycles (less than 500 thousands), a stress range up to 50 MPa can be experienced by the cable whereas for a large number of cycles (around 10 millions), the stress range experienced by the cable reduces to 2.5 MPa (Fig. 5(a)). A detailed analysis reveals that solely accounting for the uncertainties associated to the elastic modulus, pretension force, and damping ratios, large number of cycles (up to 10 millions cycles) at stress ranges below 15 MPa is induced to the cable (Fig. 5(b)). Conversely, for the case in which only the uncertainty associated to initial conditions is considered, the number of cycles range decreases (below to 4 millions cycles) but for a wider stress range (up to 50 MPa) relative to the aforementioned case (Fig. 5(c)). Results reveal in general that not accounting for the initial conditions could lead to an underestimation of the stress range experienced by the cable.

Fig. 5. Impact of uncertainties on the curve stress range - number of cycles: (a) all uncertainties are taken into account (tensile force, elastic modulus, damping ratios and initial conditions); (b) uncertainties only in tensile force, elastic modulus, and damping ratios; and (c) uncertainties only in the initial conditions. The dotted lines indicate a confidence band of 90%.

5.2 Effect of the wind speed model

As previously stated, the number of equally sized bins selected to define the wind speed histogram is 13. In this way, the typical discretization value for wind analysis of 1 m/s is obtained (Carrillo *et al*. 2014) and, as shown in Fig. 6, fitting results seem to be unaffected for wind speed histogram defined by a number of bins greater than nine. For smaller number of bins, besides of having greater values of wind speed discretization, fitting results show that the stress range experienced by the cable is greatly underestimated, specially for a number of cycles below to 3 millions in which this underestimation reaches values close to 50% of the ones provided by the high fidelity model. As it is expected, the wind speed discretization (number of bins in the interested speed range) affects the estimation of the curve stress range - number of cycles. Note that a coarse discretization (low number of bins) decreases the likelihood to excite the cable in a resonance condition; thus an underestimation of the stress range is computed. Contrary, a refined discretization eventually guarantees the cable excitation in its natural frequencies because a fine discretization resembles the real frequency content produced by the wind speed over the cable.

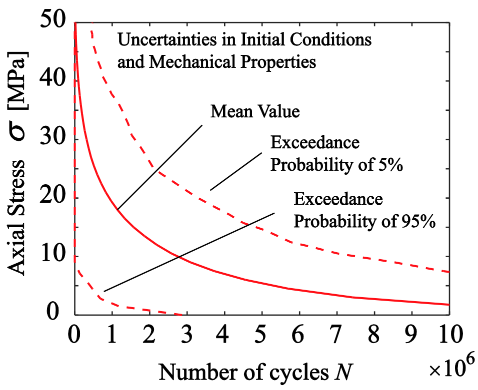

(a) all uncertainties are taken into account (tensile force, elastic modulus, damping ratios and initial conditions)

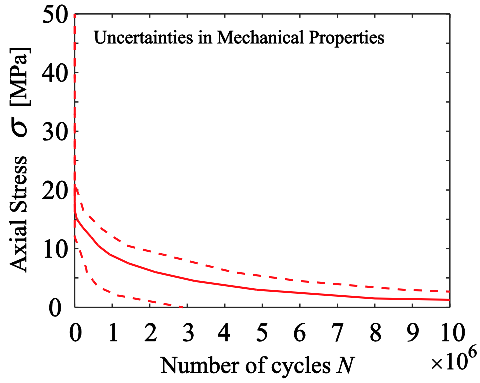

(b) uncertainties only in tensile force, elastic modulus, and damping ratios

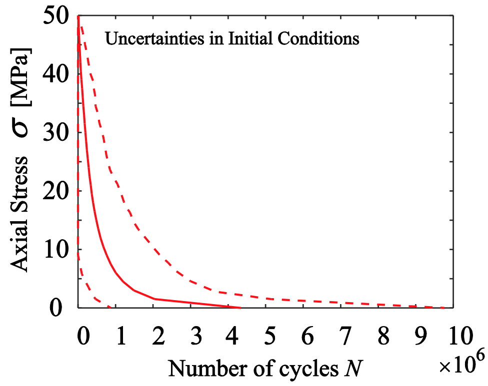

(c) uncertainties only in the initial conditions.
The dotted lines indicate a confidence band of 90%

Fig. 5 Impact of uncertainties on the curve stress range -number of cycles

Results presented in Fig. 6 correspond to mean values taking into consideration all uncertain variables (tensile force, elastic modulus, damping ratios and initial conditions).

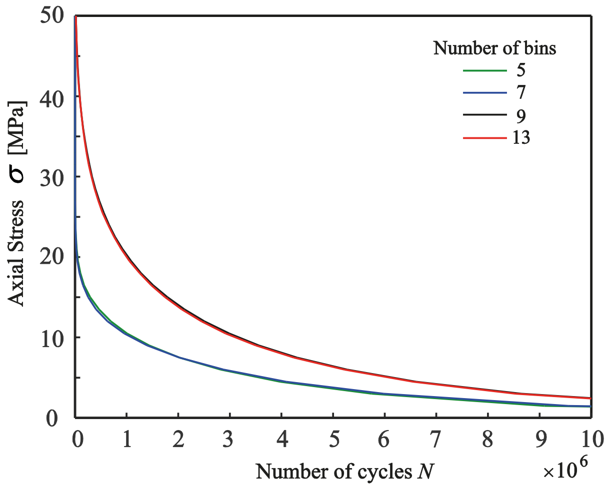

Fig. 6 Effect of the wind speed discretization on the estimation of the expected response of the cable. Mean values are reported

5.3 Effectiveness of the model in the prediction of new scenarios

The previous computation of the set $\mathbf{N}_c\left(\boldsymbol{\theta}^i \middle| v_j, t_{int}\right)$ with $\{\boldsymbol{\theta}^i,\ i=1,...,K\}$ and $\{v_j,\ j=1,...,M\}$ can be also used to evaluate different probabilistic models for the uncertain parameters and wind speed. It is of interest to present the versatility of the procedure to evaluate for example a different pretension force or a wind model with a different values of α_o and β_o. In that sense, another probabilistic model for the uncertain variables is defined as $p_{new}(\boldsymbol{\theta})$, with the only difference that the new tensile force is defined by a Gaussian distribution with mean equal to 50% greater than the nominal value and a coefficient of variation equal to 5% (Fig. 7(a)). Another wind speed model $\Pr_{new}(v)$ is also defined by using $\alpha_o = 2.5$ and $\beta_o = 1.5$ (Fig. 7(b)). Then, the cable response under the new scenario can be performed in the post processing stage by evaluating Eq. (18) but now using the new probabilistic models. Here, it is important to indicate that any new scenario runs in approximately 0.2s, which is 3000 times faster than the time required to evaluate $\mathbf{N}_c\left(\boldsymbol{\theta}^i \middle| v_j, t_{int}\right)$ for the whole set $\{\boldsymbol{\theta}^i,\ i=1,...,K\}$. Furthermore, under this scheme, the evaluation of new probabilistic scenario is independent of the model employed to estimate the dynamic response of the cable, i.e., a more complex cable model only affects the time to evaluate $\mathbf{N}_c\left(\boldsymbol{\theta}^i \middle| v_j, t_{int}\right)$ rather to affect the time to perform the post processing (where the probabilistic scenario of interest is evaluated).

Fig. 7 shows the response of the cable under different tensile force and different wind model. The solid line represents the mean value while the area between the dotted lines is associated to a confidence interval of 90%. The left figure estimate the behaviour of the cable when is subjected to the same excitation (wind model) but with a tensile force 50% greater than the nominal value. The result shows that the axial stress dramatically decreases, being the maximum axial stress around 4 times lower than the nominal case. On the other hand, the confidence interval of 90% is also reduced, in part as a consequence of the reduction in the coefficient of variation associated to the tensile force. The increment in the tensile force also increases the natural frequencies of the cable, thus the likelihood that the wind speed excites the lower natural frequencies is decreased. If the properties of the cable are now kept and the wind model is changed (Fig. 7(b)) occurs a different situation. In this case, the wind speed model only changes the probability to have a particular speed. In that sense, the cable has the same likelihood to be excited at its natural frequencies but it will be in resonance during different amount of time. This situation is evident in Fig. 7(b), where the maximum axial stress is the same for both wind models employed.

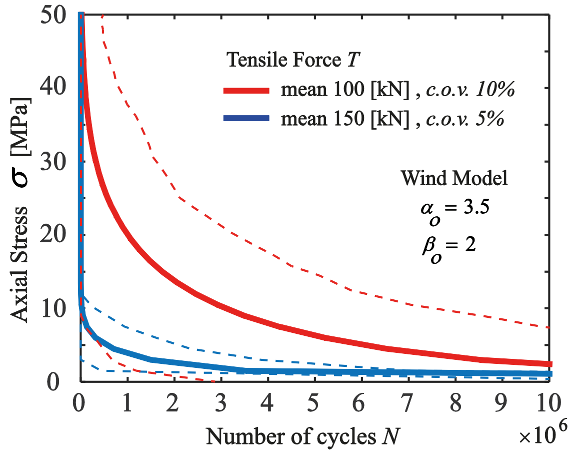

(a) Shows the expected response due to a greater tensile force (150kN and 5% of coefficient of variation)

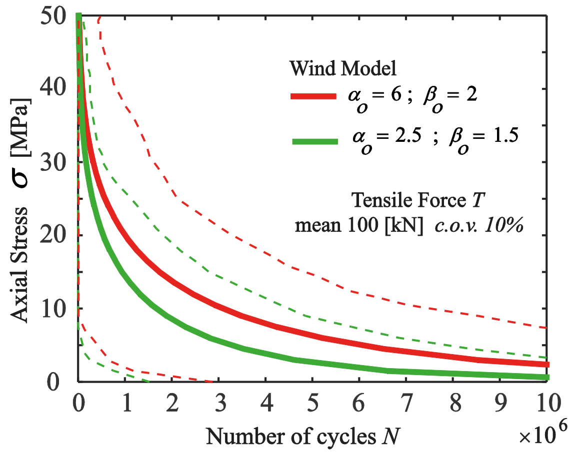

(b) Expected response under a different wind model (Weibull distribution with $\alpha_o = 2.5$ and $\beta_o = 1.5$)

Fig. 7 Estimation of the cable response under different scenarios.

6. Conclusions

An efficient framework to estimate the number of stress cycles of cables under wind-induced vibrations due to vortex shedding is presented. The procedure takes into account the uncertainties associated to the elastic modulus, tensile force, damping, initial conditions, and wind speed. Any given probabilistic density function is admitted to describe the uncertain variables. The algorithm relies on the use of Monte Carlo simulations to estimate the stress cycles and the concept of importance sampling to allow the computation of different probabilistic models without a significant computational burden. An enriched cable model is established allowing the adequate estimation of its curvature. The cable model also incorporates the effect of internal wires by properly accounting their inertias contribution and their helix angles.

The applicability of the proposed framework is shown by estimating the stress range-number of cycles curves relative to the vortex shedding-induced vibrations on a 15 mm diameter high-strength steel strand. In this case study analysis, uncertainties associated to the elastic modulus, tensile force, damping ratios and initial conditions are considered. The results indicate that not accounting for the initial conditions uncertainties or using a coarse wind speed discretization (less than 9 bins for the study case) could lead to an underestimation of the stress range experienced by the cable. On the other hand, a finer discretization (greater than 9 bins for the study case) eventually resembles the real wind speed frequency content exciting the cable in its natural frequencies, which induces higher stress ranges developed by the cable. In addition, uncertainties in the elastic modulus, tensile force, damping ratios do not significantly affect the estimated stress range-number of cycles curve of the cable.

A key aspect of the proposed framework is its computational efficiency when parametric studies, impact of using different probabilistic models for the uncertain parameters and wind speed, are carried out. This advantage (computational efficiency) relies on the independency of the evaluation of the dynamic response using the sampling density and the probabilistic models of interest in which the algorithm is based on. Furthermore, the algorithm can be implemented in a sequential fashion such that, along with a frequent parameter identification (cable´s properties), bending fatigue progression can be evaluated by a direct comparison with a S-N curve.

Acknowledgments

The authors would like to acknowledge and thank the sponsor of this work University of Chile (Insertion into Research Project) for its financial support.

References

ABAQUS, F. (1996), User's manual, version 5.5. Commer. Softw. Package Habitt Karlsson Sorensen Inc 1080.

An1a, Y., Wang, C., Li, S. and Wang, D. (2016), "Galloping of steepled main cables in long-span suspension bridges during construction", *Wind Struct*., **23**(6), 595-613.

Argentini, T., Rosa, L. and Zasso, A. (2016), "Wind-induced vibrations of the stay cables of a roundabout flyover: Assessment, repair, and countermeasures", *J. Perform. Constr. Fac*., **30**(6), 04016046.

Bean, M.J. (2006), Bending Fatigue Performance of Small-Scale Stay Cables. Master's thesis, the University of Texas at Austin, May.

Beltrán, J.F. and De Vico, E. (2015), "Assessment of static rope behavior with asymmetric damage distribution", *Eng. Struct*., **86**, 84-98.

Beltrán, J.F. and Vargas, D. (2012), "Effect of broken rope components distribution throughout rope cross-section on polyester rope response: Numerical approach", *Int. J. Mech. Sci*., **64**(1), 32-46.

Carberry, J., Sheridan, J. and Rockwell, D. (2001), "Forces and wake modes of an oscillating cylinder", *J. Fluid. Struct*., **15**(3-4), 523-532.

Carrillo, C., Cidrás, J., Díaz-Dorado, E. and Obando-Montaño, A.F. (2014), "An approach to determine the Weibull parameters for wind energy analysis: the case of Galicia (Spain)", *Energies*, **7**, 2676-2700.

Carta, J.A., Ramirez, P. and Velazquez, S. (2009), "A review of wind speed probability distributions used in wind energy analysis: Case studies in the Canary Islands", *Renew. Sust. Energ. Rev*., **13**(5), 933-955.

Chaplin, C.R. (1999), "Torsional failure of a wire rope mooring line during installation in deep water", *Eng. Fail. Anal*., **6**(2), 67-82.

Chaplin, C.R. (2005), The fatigue and degradation mechanisms of hoisting ropes, in: Hoist and Haul Conference Perth, WA., 5-7.

Chiodo, E. and De Falco, P. (2016), "Inverse Burr distribution for extreme wind speed prediction: Genesis, identification and estimation", *Electr. Pow. Syst. Res*., **141**, 549-561.

Cluni, F., Gusella, V. and Ubertini, F. (2007), "A parametric investigation of wind-induced cable fatigue", *Eng. Struct*., **29**, 3094-3105.

Comanducci, G., Ubertini, F. and Materazzi, A.L. (2015), "Structural health monitoring of suspension bridges with features affected by changing wind speed", *J. Wind Eng. Ind. Aerod*., **141**, 12-26.

Facchinetti, M.L., De Langre, E. and Biolley, F. (2004), "Coupling of structure and wake oscillators in vortex-induced vibrations", *J. Fluid. Struct*., **19**(2), 123-140.

Fadel, A.A., Rosa, D., Murça, L.B., Fereira, J.L.A. and Araújo, J.A. (2012), "Effect of high mean tensile stress on the fretting fatigue life of an Ibis steel reinforced aluminium conductor", *Int. J. Fatigue*, **42**, 24-34.

Flamand, O., De Oliveira, F., Stathopoulos-Vlamis, A. and Papanikolas, P. (2014), "Conditions for occurrence of vortex shedding on a large cable stayed bridge: Full scale data from monitoring system", *J. Wind Eng. Ind. Aerod*., **135**, 163-169.

Foster, G.P. (2002), "Advantages of fiber rope over wire rope", *J. Ind. Text*., **32**, 67-75.

Ge, Y., Chang, Y., Xu, L. and Zhao, L. (2018), "Experimental investigation on spatial attitudes, dynamic characteristics and environmental conditions of rain–wind-induced vibration of stay cables with high-precision raining simulator", *J. Fluid. Struct*., **76**, 60-83.

Giaccu, G.F., Barbiellini, B. and Caracoglia, L. (2015), "Stochastic unilateral free vibration of an in-plane cable network", *J. Sound Vib*., **340**, 95-111.

Grouthier, C., Michelin, S., Bourguet, R., Modarres-Sadeghi, Y. and De Langre, E. (2014), "On the efficiency of energy harvesting using vortex-induced vibrations of cables", *J. Fluid. Struct*., **49**, 427-440.

Guérard, S. (2011), Power line conductors, a contribution to the analysis of their dynamic behaviour. Université de Liège, Belgique.
Hallquist, J.O. (2006), LS-DYNA theory manual, Livermore Softw. Technol. Corp. 3, 25-31.
Harper, B.A., Kepert, J.D. and Ginger, J.D. (2010), Guidelines for converting between various wind averaging periods in tropical cyclone conditions, World Meteorol. Organ. WMOTD 1555.
Jacinto, L., Pipa, M., Neves, L.A. and Santos, L.O. (2012), "Probabilistic models for mechanical properties of prestressing strands", *Constr. Build. Mater*., **36**, 84-89.
Kalombo, R.B., Araújo, J.A., Ferreira, J.L.A., Da Silva, C.R.M., Alencar, R. and Capra, A.R. (2016), "Assessment of the fatigue failure of an All Aluminium Alloy Cable (AAAC) for a 230kV transmission line in the Center-West of Brazil", *Eng. Fail. Anal*., **61**, 77-87.
Knapp, R.H. (1998), Cable CAD User Manual. Knapp Eng. Inc.
Kumarasena, S., Jones, N.P., Irwin, P. and Taylor, P. (2005), Wind induced vibration of stay cables.
Kwofie, S. (2001), "An exponential stress function for predicting fatigue strength and life due to mean stresses", *Int. J. Fatigue*, **23**(9), 829-836.
Li, S.Y., Wu, T., Li, S.K. and Gu, M. (2016), "Numerical study on the mitigation of rain-wind induced vibrations of stay cables with dampers", *Wind Struct*., **23**(6), 615-639.
Lipecki, T. and Flaga, A. (2013), "Vortex excitation model. Part I. mathematical description and numerical implementation", *Wind Struct*., **16**(5), 457-476.
Luongo, A. and Zulli, D. (2013), Mathematical models of beams and cables, John Wiley & Sons.
Lutes, L.D. and Sarkani, S. (1997), Stochastic analisys of structural and mechanical vibrations, Prentice Hall.
Matsumoto, M., Shirato, H., Yagi, T., Goto, M., Sakai, S. and Ohya, J. (2003), "Field observation of the full-scale wind-induced cable vibration", *J. Wind Eng. Ind. Aerod*., **91**(1-2), 13-26.
Nemov, A.S., Boso, D.P., Voynov, I.B., Borovkov, A.I. and Schrefler, B.A. (2010), "Generalized stiffness coefficients for ITER superconducting cables, direct FE modeling and initial configuration", *Cryogenics*, **50**(5), 304-313.
Qi, G. (2013), Computational Modeling for Stress Analysis of Overhead Transmission Line Stranded Conductors Under Design and Fretting Fatigue Conditions, McGill University.
Raeesi, A., Cheng, S. and Ting, D.S. (2014), "A two-degree-of-freedom aeroelastic model for the vibration of dry cylindrical body along unsteady air flow and its application to aerodynamic response of dry inclined cables", *J. Wind Eng. Ind. Aerod*., **130**, 108-124.
Sarkar, A. and Taylor, R.E. (2002), "Dynamics of mooring cables in random seas", *J. Fluid. Struct*., **16**(2), 193-212.
Seguro, J.V. and Lambert, T.W. (2000), "Modern estimation of the parameters of the Weibull wind speed distribution for wind energy analysis", *J. Wind Eng. Ind. Aerod*., **85**(1), 75-84.
Shinde, V., Jha, J., Tewari, A. and Miashra, S. (2018), "Modified rainflow counting algorithm for fatigue life calculation", *Proceedings of Fatigue, Durability and Fracture Mechanics*. 381-387.
Wang, D., Chen, X. and Li, J. (2017), "Prediction of wind-induced buffeting response of overhead conductor: Comparison of linear and nonlinear analysis approaches", *J. Wind Eng. Ind. Aerod*., **167**, 23-40.
Winkler, J., Georgakis, C.T. and Fischer, G. (2015), "Fretting fatigue behavior of high-strength steel monostrands under bending load", *Int. J. Fatigue*, **70**, 13-23.
Wood, S.L. and Frank, K.H. (2009), "Experimental investigation of bending fatigue response of grouted stay cables", *J. Bridge Eng*., **15**(2), 123-130.

CC